3-D Inversion of Induced Polarization Data

Li, Y.[1], and Oldenburg, D.W.[1]

1. Geophysical Inversion Facility, University of British Columbia, Vancouver, B.C.

ABSTRACT

We present an algorithm for inverting induced polarization data acquired in a three-dimensional environment using the linearized equation for the IP response. The inverse problem is solved by minimizing an objective function of the chargeability model subject to data and positivity constraints. The minimization is carried out using a logarithmic barrier method. We study the effect of different approximations to the background conductivity in the IP inversion and demonstrate that good IP results are obtainable without using the best conductivity estimate derived from full 3-D inversion of the DC data. We also study the joint use of surface and borehole data in improving the resolution of the recovered chargeability models, and demonstrate that the joint inversion of surface and cross-hole data produces chargeability models superior to those obtained from inversions of individual data sets.

INTRODUCTION

In an earlier paper (Oldenburg and Li, 1994), we presented three different approaches for inverting induced polarization (IP) data and illustrated them using 2-D examples. IP data can be inverted by a linearized approach, by performing two DC resistivity inversions, or by a full nonlinear inversion. These methods are general and applicable to either 1-D, 2-D, or 3-D problems, but their implementation in 3-D poses numerical and computational challenges. In this paper, we address the extension of our algorithm developed in that paper to the 3-D environment. Here we choose to work with the linearized approach and implement it for general electrode configurations. When the magnitude of the chargeability is moderate, the secondary potential ϕ_s measured in an IP experiment is linearly related to the intrinsic chargeability by (e.g., Siegel, 1959),

$$\phi_{si} = \sum_{j=1}^{M} -\eta_j \frac{\partial \phi_{\eta i}}{\partial \ln \sigma_j} \equiv \sum_{j=1}^{M} \eta_j J_{ij}^{\phi} \qquad [1]$$

where ϕ_η is the total potential measured in the presence of the IP effect, σ_j and η_j are respectively the conductivity and chargeability value in the jth region, and J_{ij}^{ϕ} is the sensitivity of the secondary potential. When the measured total potential is not approaching zero, an apparent chargeability η_a can be defined as the ratio of the secondary potential to the total potential, and the linear relation in Equation [1] becomes

$$\eta_{ai} = \sum_{j=1}^{M} -\eta_j \frac{\partial \ln \phi_{\eta i}}{\partial \ln \sigma_j} \equiv \sum_{j=1}^{M} \eta_j J_{ij}^{\eta} \qquad [2]$$

where J_{ij}^{η} is the corresponding sensitivity.

Apparent chargeability is the preferred form of IP data and it is well defined in the surface and some downhole surveys. However, in the cross-hole experiments using dipole sources or receivers, the electric field often changes sign along the borehole and the measured total potential differences can approach zero. These near-zero potentials make both the apparent chargeability and its sensitivity undefined in Equation [2]. It is therefore necessary to use the secondary potential as data directly.

Given a set of measured IP data, inversion of either Equation [1] or [2] allows the recovery of the intrinsic chargeability model. Since the true conductivity structure is unknown in practical applications, an approximation to it is substituted in the calculation of the sensitivities. This approximation is usually obtained by inverting the accompanying DC potential data. Thus, the IP inverse problem is a two-stage process. In the first stage, an inverse problem is solved to recover a background conductivity model from the DC data. This model is then used to generate the sensitivity for the IP inversion and a linear inverse problem is solved to obtain the chargeability model.

FORMULATION OF THE INVERSION

Assume we have a set of N IP data, which can be apparent chargeabilities or secondary potentials. To invert these data for a 3-D model of chargeability, we first use an orthogonal mesh to divide the model region into M cells and assume a constant chargeability value in each cell. The data are formally related to the chargeabilities in the cells by the relation in Equations [1] and [2],

$$\vec{d} = \mathbf{J}\vec{\eta} \qquad [3]$$

where the data vector $\vec{d} = (d_1, \ldots, d_N)^T$ and the model vector $\vec{\eta} = (\eta_1, \ldots, \eta_M)^T$. $\mathbf{J}$ is the sensitivity matrix corresponding to the data, whose elements $\mathbf{J}_{ij}$ are calculated from the assumed approximation to the background conductivity.

In "Proceedings of Exploration 97: Fourth Decennial International Conference on Mineral Exploration" *edited by* A.G. Gubins, 1997, p. 549–552

The number of model cells is generally far greater than the number of data available, and thus an underdetermined problem is solved and it is necessary to obtain the solution by minimizing an objective function of the model subject to the data constraints in Equation [3].

We use a model objective function that is similar to that for the 2-D case but has an extra derivative term in the third dimension,

$$\psi(\eta) = \alpha_s \int_V w_s(\eta-\eta_0)^2 dv + \alpha_x \int_V w_x \left\{\frac{\partial(\eta-\eta_0)}{\partial x}\right\}^2 dv + \alpha_y \int_V w_y \left\{\frac{\partial(\eta-\eta_0)}{\partial y}\right\}^2 dv + \alpha_z \int_V w_z \left\{\frac{\partial(\eta-\eta_0)}{\partial z}\right\}^2 dv \quad [4]$$

where η_0 is a reference model. The functions w_s, w_x, w_y, and w_z are spatially dependent weighting functions while α_s, α_x, α_y, and α_z are coefficients which affect the relative importance of the different components. For numerical solution, Equation [4] is discretized using the finite difference approximation.

The data constraints are satisfied by requiring that the total misfit between the observed and predicted data be equal to a target value. We measure the data misfit using the function

$$\psi_d = \sum_{i=1}^{N} \left(\frac{d_i^{obs} - d^{pre}}{\delta_i} \right)^2 \quad [5]$$

where the δ_i is the standard deviation of the estimated error of each datum.

The total objective function to be minimized is formed by introducing a tradeoff parameter μ,

$$\psi = \psi_d + \mu\psi(\vec{\eta}) \quad [6]$$

Minimization of Equation [6] subject to the constraint that the chargeability be positive using any optimization technique yields the desired chargeability model. The positivity constraint is required since the chargeability is defined in the range (0,1). We choose to use an interior point method in which the positivity is implemented by including a logarithmic barrier term in the objective function:

$$\psi = \psi_d + \mu\psi(\vec{\eta}) - \lambda \sum_{j=1}^{M} \ln(\eta_j) \quad [7]$$

where λ is the barrier parameter. The minimization starts with a model whose elements are all well above the zero bound and a large value for λ. It then iterates to the final solution as λ is decreased towards zero. The tradeoff parameter μ is fixed during the minimization.

We illustrate our algorithm using a test model composed of five anomalous rectangular prisms embedded in a uniform halfspace. The geometry of the model is shown in Figure 1. There are three surface prisms simulating near surface distortions, and two buried prisms simulating deeper targets. DC resistivity and IP data from both surface and cross-hole experiments have been computed.

The surface experiment is carried out using a pole-dipole array with a=50 m and n=1, 6. There are seven traverses spaced 100 m apart in both east-west and north-south directions. The resulting data set consists of 1,500 observations. We have contaminated the data with a minimum of 2% independent Gaussian noise. We first perform a full non-linear inversion of the DC resistivity data and then use the resultant conductivity in the inversion of the IP data. The inverted chargeability model is shown in Figure 2 by one cross-section and two plan-sections. The model yields a good representation of the true anomalous chargeability zones. The definition is clear near the surface and becomes more diffused at depth. This is an expected result when surface data are inverted.

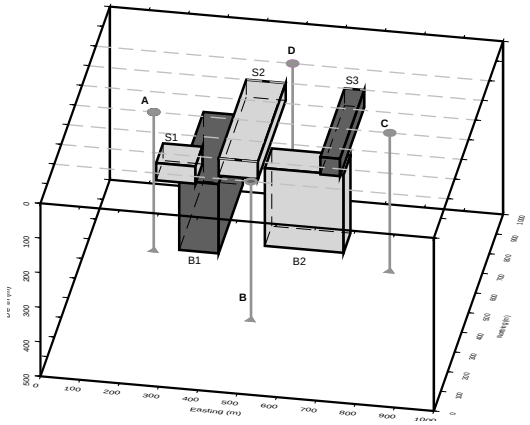

Figure 1: *Perspective view of the five-prism model. Seven surface traverses in the east-west direction and four boreholes are also shown. For clarity, seven traverses in the north-south direction are not shown. The prisms S1, S2, and B2 are more conductive and S3 and B1 are more resistive than the background. All five prisms are chargeable.*

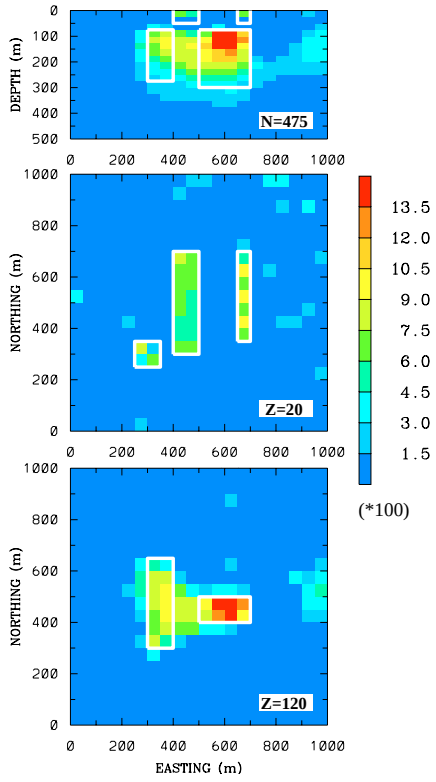

Figure 2: *The chargeability model recovered from inversion of surface data. The conductivity from full 3-D DC inversion is used to calculate sensitivities. The position of the true prisms are indicated by the white lines.*

INVERSION USING APPROXIMATE CONDUCTIVITY MODELS

The full non-linear inversion of 3-D DC resistivity data is a costly undertaking, especially when the recovery of the conductivity model is but an intermediate step towards the end goal of recovering the chargeability model. More importantly, good IP inversion results are often obtained by using other less rigorous approximations to the conductivity. Our experience with 2-D inversions (Oldenburg and Li, 1994) has shown that good first-order results concerning the chargeability distribution can often be obtained by approximating the earth using a homogeneous conductive halfspace. This suggests that reasonable recovery of a chargeability model could be achieved by using intermediate approximations between these two end members corresponding to a uniform halfspace and the conductivity model recovered from a full non-linear 3-D DC inversion. Thus, the accurate recovery of the background conductivity via a full 3-D inversion of DC data may not be necessary.

We have examined five different approximations, including the conductivity obtained from full 3-D inversions used in the preceding section. These approximations are briefly discussed below.

1. A uniform halfspace: This is the simplest approximation and no inversion of DC data is involved.
2. One-pass approximate 3-D inversion: This is the conductivity model obtained from a linear inversion of the DC data assuming that the actual conductivity consists of weak perturbations of a uniform halfspace.
3. Composite 2-D inversions: Independent 2-D inversions are carried out along each line so that a 2-D model is generated. The 2-D models are then combined to form a 3-D representation of the true conductivity.
4. Limited 3-D AIM updates: The one-pass 3-D inversion is used to carry out a small number of AIM updates to produce an approximate conductivity model.
5. Full 3-D inversion: The conductivity model obtained from complete AIM updates or from linearized inversions.

We have inverted the surface IP data from our test model using these different conductivity approximations. The results are compared with the true model in Figure 3. Each panel in that figure is the cross-section of the recovered chargeability model at N=475 m, which passes through four of the five prisms. All five models recover the essential features of the true model and they present a general trend of improvement as the approximation to the background conductivity improves.

JOINT INVERSION OF SURFACE AND BOREHOLE DATA

Crosshole data have been used in the effort to achieve high resolution images of the subsurface structure obtainable from DC/IP experiments. However, although crosshole data are very sensitive to the vertical variation, they have rather poor sensitivity to the lateral variation because the data have limited spatial distribution and the array separation is restricted to a small range. Surface data, however, usually have good areal coverage and therefore possess much better resolving power for determining lateral variation in the subsurface structure. The surface data can provide good complementary information to the crosshole data if the targets are within the depth of penetration of the surface arrays. Joint inversion of these two data sets will improve the resolution of the recovered chargeability model.

We have placed four vertical boreholes around the anomalous region in the test model and the locations are shown in Figure 1. Crosshole

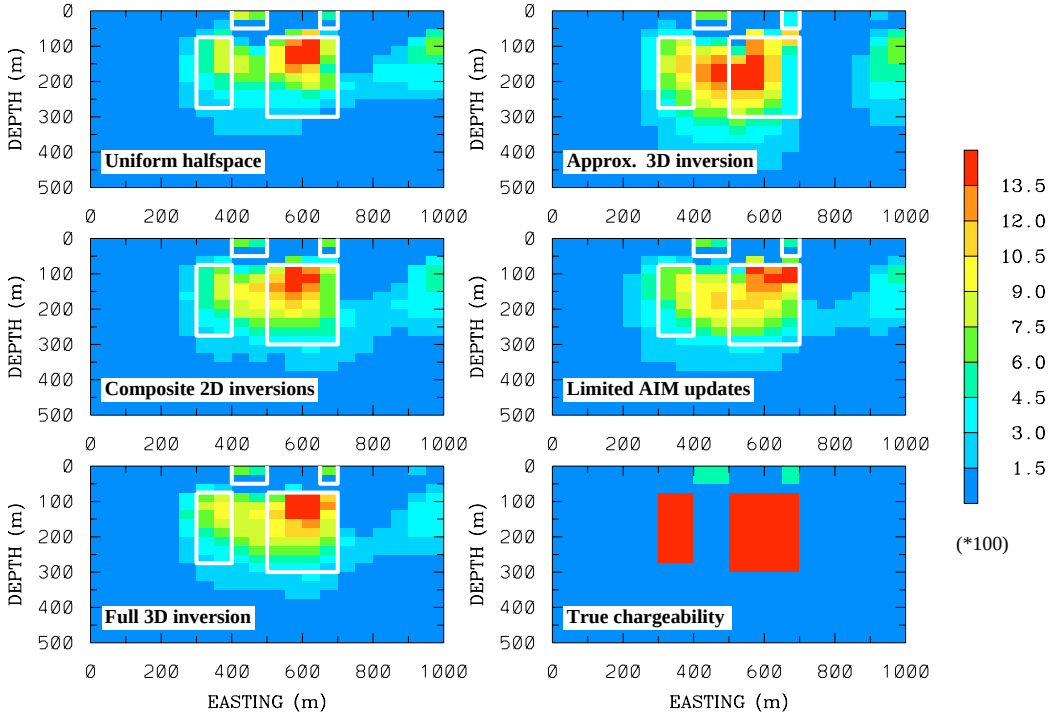

Figure 3: *Comparison of chargeability models recovered from the 3-D inversion of surface IP data using five different approximations to the background conductivity. The process by which each conductivity approximation is obtained is shown in each panel. The lower-right panel is the true chargeability model.*

pole-dipole data, with a receiver-dipole length of 50 m and 2% of Gaussian noise, have been simulated. Both source and receiver are placed every 25 m along the borehole; only one borehole in any pair of boreholes is used as the source hole and the reverse configuration switching the source and receiver holes is not used. A total of 1,530 observations are generated. In the following, we first apply our 3-D algorithm to the crosshole data from the five-prism model. We then jointly invert the surface and crosshole data and demonstrate that the resultant model is superior to the model obtained from the individual inversion.

Figure 4 shows the chargeability model recovered from the crosshole data alone. (In this and the following joint inversion, we have used the conductivity model recovered from full 3-D inversion of the corresponding DC data.) The definition of the anomalous prisms is rather poor, although the larger ones are all identified to a certain extent. There is excessive structure in the region immediately surrounding the boreholes. Figure 5 displays the chargeability recovered from the joint inversion of surface and crosshole data. It shows dramatic improvement over the models from individual inversions in Figures 2 and 4. The most noticeable feature is the clear image of the two separate buried targets.

DISCUSSION

We have developed a 3-D IP inversion algorithm that is applicable to data acquired using arbitrary electrode configurations. We represent the model by a large number of cells of constant conductivity and chargeability and obtain the solution by minimizing an objective function. The interior point method with a logarithmic barrier is shown to be an efficient approach for large 3-D inversion with positivity constraint. Several different, inexpensive approximations to the background conductivity used in sensitivity calculation have been shown to produce reasonable IP inversion results. Therefore, the costly full 3-D inversion of DC data does not seem to be a prerequisite to a high quality 3-D IP inversion. Lastly, application of our inversion algorithm to joint surface and crosshole data has demonstrated that the inversion of these two complementary data sets can greatly improve the resolution of the inverted chargeability model.

ACKNOWLEDGEMENTS

This work was supported by an NSERC IOR grant and an industry consortium "Joint and Cooperative Inversion of Geophysical and Geological Data." Participating companies are Placer Dome, BHP Minerals, Noranda Exploration, Cominco Exploration, Falconbridge, INCO Exploration & Technical Services, Hudson Bay Exploration and Development, Kennecott Exploration Company, Newmont Gold Company, WMC Ltd., and CRA Exploration Pty.

REFERENCES

Oldenburg, D. W. and Li, Y., 1994. Inversion of induced polarization data: *Geophysics*, **59**, 1327-1341.

Siegel, H. O., 1959. Mathematical formulation and type curves for induced polarization: *Geophysics*, **24**, 547-565.

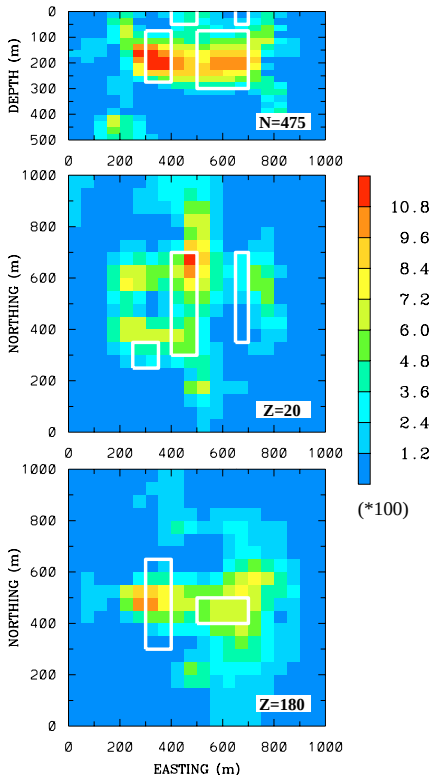

Figure 4: *Chargeability model recovered from crosshole data alone.*

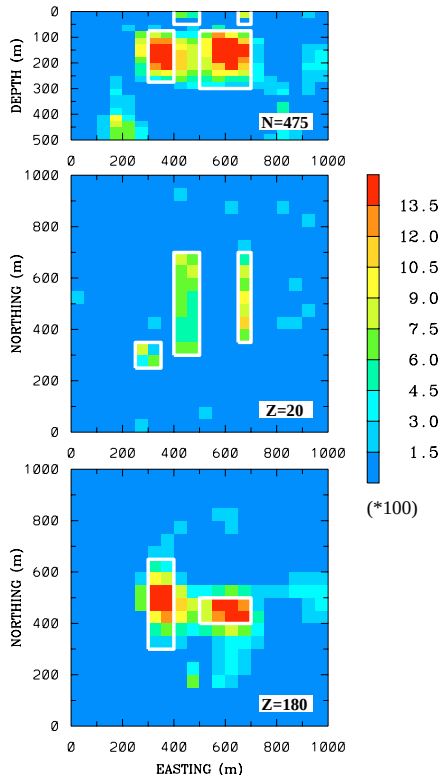

Figure 5: *Chargeability model recovered from the joint inversion of surface and crosshole data.*